Humidity-dependent mechanical and adhesive properties of *Arachnocampa tasmaniensis* capture threads

D. Piorkowski[1] (iD), T. A. Blackledge[2], C.-P. Liao[1], N. E. Doran[3], C.-L. Wu[4], S. J. Blamires[5] & I.-M. Tso[1,6]

1 Department of Life Science, Tunghai University, Taichung, Taiwan
2 Department of Biology, Integrated Bioscience Program, The University of Akron, Akron, OH, USA
3 Bookend Trust, Hobart, TAS, Australia
4 Center for Measurement Standards, Industrial Technology Research Institute, Hsinchu, Taiwan
5 Evolution and Ecology Research Centre, University of New South Wales, Sydney, NSW, Australia
6 Center for Tropical Ecology and Biodiversity, Tunghai University, Taichung, Taiwan

Abstract

Bioluminescent glow-worms (*Arachnocampa* spp.) capture prey in glue-coated silk capture threads hung from their nests on damp cave and wet forest substrates. In a dry environment, these animals are very susceptible to desiccation as their bodies can become life threateningly dry and their silk has been anecdotally observed to become non-sticky. Water has a plasticizing effect on the structural proteins of several invertebrate silks, including those used in caddisfly nets, mussel byssus and spider webs. Moreover, water facilitates interfacial adhesion by spreading adhesive biomolecules in functionally analogous velvet worm slime and spider silk glue. We tested the effects of water on the mechanics and adhesion of *Arachnocampa tasmaniensis* capture threads sampled within damp caves. We found that threads tested at high humidity were three times more compliant and over 10-fold more extensible than those tested at low humidity (30% RH). We also found the threads to be significantly more adhesive in high humidity with force at detachment increasing two orders of magnitude and work of adhesion increasing by five orders of magnitude compared to threads tested at low humidity. Our results unequivocally demonstrate that *A. tasmaniensis* capture thread functionality is dependent upon exposure to high humidity. Our results both confirm previous reports and indicate that the foraging habitat of these animals is restricted to caves and cave-like environments, such as wet forests.

Introduction

The larval stage of cave-dwelling insects of the genus *Arachnocampa* (Diptera: Keroplatidae) or 'glow-worms' produce a bioluminescent light from their abdomens that attracts insect prey in an attempt to capture them in their silken nests (Fig. 1; Pugsley, 1984; Broadley & Stringer, 2001; Willis, White & Merritt, 2011). These nests are composed of sticky capture threads secreted by the glow-worm that hang from a tubular retreat on the cave ceiling or other suitable substrates within damp caves or nearby wet forests (Meyer-Rochow, 2007; Merritt & Patterson, 2017). In their native high humidity environment (90–100% RH), the threads are highly extensible, consisting of two or more silk fibers coated in a sticky, viscous glue (Meyer-Rochow, 2007; Von Byern *et al.*, 2016). However, anecdotal observations (Meyer-Rochow, 2007; Walker *et al.*, 2015; Von Byern *et al.*, 2016) report extreme susceptibility of the glow-worm capture threads, as well as

their bodies, to desiccation. These studies observed silk strands to become brittle and non-adhesive in dry environments, alluding to the possibility that their prey catching functionality is dependent upon water.

Many amorphous biomolecules, such as silk and biofilm proteins (Blasi *et al.*, 2005; Vollrath & Porter, 2006), and numerous sugars like maize starch (Mathew & Dufresne, 2002) and trehalose (Cordone, Cottone & Giuffrida, 2007), undergo a glass-to-rubber transition above a certain temperature (T_g). The presence of water can greatly reduce T_g as water is a known plasticizer and promotes molecular mobility (Sperling, 2005). Not surprisingly, many invertebrate silks, such as silkworm cocoon silk (Pérez-Rigueiro *et al.*, 2000; Plaza *et al.*, 2008), lacewing silk egg stalks (Bauer *et al.*, 2012), caddisfly net silk (Tsukada *et al.*, 2010) and various spider silks (Gosline, Denny & DeMont, 1984; Shao, Young & Vollrath, 1999) as well as mussel byssus (Smeathers & Vincent, 1979; Troncoso, Torres & Grande, 2008), become rubberized when

Figure 1 Flying insect caught in sticky capture thread of *Arachnocampa tasmaniensis* as the glow-worm larvae hauls its prey up for consumption. Copyright: SIXTEEN LEGS/Bookend Trust, photo credit: Joe Shemesh. [Colour figure can be viewed at zslpublications.onlinelibrary.wiley.com]

exposed to water, as stiffness (Young's modulus) is reduced and extensibility (breaking strain) is increased. This softening effect is believed to be the result of water molecules disrupting intermolecular hydrogen bonds (Termonia, 1994; Bauer *et al.*, 2012). In spider and silkworm silks, this disruption also causes fiber shrinkage, a phenomenon known as supercontraction, of up to 50% in some cases, as the protein structures conform into a lower energy state (Grubb & Ji, 1999; Jelinski *et al.*, 1999; Plaza *et al.*, 2008; Fu, Porter & Shao, 2009; Boutry & Blackledge, 2010). In determining precisely how water influences the tensile performance of *Arachnocampa* capture threads it is also important to identify whether water induces a contraction response to provide a first step toward understanding the molecular mechanisms underpinning the performance of this fascinating biomaterial.

Arachnocampa capture threads are coated in an aqueous glue that forms droplets that intersperse along the fiber in a way that superficially resembles the spiral threads of spider orb webs (Meyer-Rochow, 2007; Walker *et al.*, 2015). This glue appears to be highly responsive to atmospheric water as droplets dry out at humidities of <80% RH but can be rehydrated when exposed to 100% RH (Von Byern *et al.*, 2016). By comparison, spider glue utilizes organic and inorganic salts to uptake and maintain atmospheric water, which facilitates dissolution and spreading of adhesive glycoproteins (Sahni *et al.*, 2014; Amarpuri *et al.*, 2015). The gluey silk of several species of orb web spiders appears to have adhesive properties that are optimized for the specific native humidity within their natural habitats (Opell, Karinshak & Sigler, 2013; Baba *et al.*, 2014; Amarpuri *et al.*, 2015). While the specific chemical composition of *Arachnocampa* capture glue likely differs from that of spider glue (Von Byern *et al.*, 2016), it is possible that their adhesive performance is optimized to the high humidity (90–100% RH) of its native cave or wet forest environment.

Here, we tested the hypothesis that glow-worm capture threads are functionally optimized to the high humidity cave environment by performing mechanical and adhesion tests on capture silk threads of the glow-worm *Arachnocampa tasmaniensis* at high (>90% RH) and low (30% RH) humidities. We also tested whether the glow-worm silks contracted when exposed to high humidity to indirectly test for evidence of the presence of intermolecular bonds that may be responsible for differences in mechanical performance in different humidities.

Materials and methods

Collection, transportation and characterization of glow-worm larvae capture silk

We collected adhesive capture silk threads from glow-worm nests from the ceilings of Mystery Creek and Bradley Chesterman caves, in Southwest National Park, Tasmania, Australia, in September 2015 and October 2017. Collection was conducted as permitted by the Tasmanian Department of Primary Industries, Parks, Water and the Environment (permit No. FA15189 and FA17188, respectively). We cut clean capture threads hanging vertically from the nest, using scissors, and attached them to strips of paper with 10 × 10 mm square gaps so that all segments collected measured 10 mm in length. The naturally adhesive properties of the capture threads provided temporary attachment to the paper strips until they were permanently affixed with water-resistant wood working glue 24 h later at the University of Tasmania, Hobart. Samples were stored in microscope slide boxes in controlled laboratory settings at ambient temperature (20°C) and humidity (60% RH).

The capture silk threads were transported to the University of Akron, Akron, Ohio, USA in 2015 and the Industrial Technology Research Institute, Hsinchu, Taiwan in 2017, within 2 weeks of collection for laboratory testing. Contamination was low as samples were sealed in airtight transport boxes. Several capture threads became dry and brittle during travel to the USA and broke easily, which were discarded. We were careful to expose all samples to identical conditions while collecting, handling, traveling with and testing the threads.

We subjected 74 thread segments from 22 individuals to polarized light microscopy, adhesion and dry and wet tensile testing. We used identical Nanobionix (MTS, Oak Ridge, TN, USA) tensile testers for mechanical and adhesion testing at both institutions with similarly designed environmental chambers. During adhesion and tensile tests, threads were exposed to the highest humidity levels (*c.* >90% RH, high humidity) attainable by our chambers, and ambient humidity (30% RH, low humidity). We pre-tested both machines and found similar performances for standard dry and wet tensile tests. Accordingly, we combined the datasets collected for measurements on both machines.

Polarized light microscopy

To determine the number of fibers present within a single capture thread and their respective diameters, we adhered threads to a

glass slide and dispersed the droplet coating surrounding the internal fibers using water to acquire an undistorted or magnified image via polarized light microscopy (Blackledge, Cardullo & Hayashi, 2005). Our methods were identical to those described by Swanson, Blackledge & Hayashi (2007), who determined diameters of spider gluey silk. We observed seven samples, one each from different individual larvae, and determined that the capture threads have two adjacent fibers in all samples (see Fig. 2). Cross-sectional area was therefore calculated as $A = 2^{0.5} \pi(d/2)^2$, with d being the diameter of one fiber.
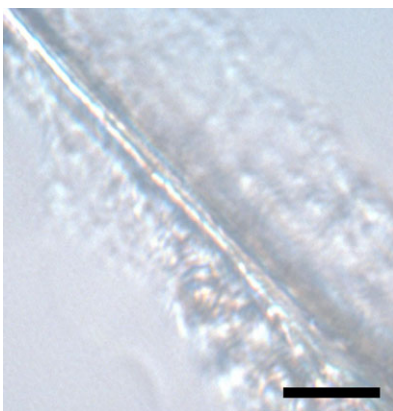
This method of measuring silk thread diameters renders samples unusable for further testing. Preliminary data indicated that diameters of threads from individuals arbitrarily assigned to wet and dry treatments did not differ, (95% HPD intervals = −0.26 to 0.21 μm, $P_{MCMC} = 0.88$). Therefore, we established an average diameter used for samples from all other individuals ($N = 7$) in an effort to maximize silk samples available for testing.

Testing for contraction at high humidity

We used five capture thread samples from different individuals to test for the presence of contraction during exposure to high humidity, as has been described for spider dragline silks (Agnarsson *et al.*, 2009; Boutry & Blackledge, 2010). Capture threads were mounted on the tensile tester within an environmental chamber at ~20°C and stretched until taut (15 μN) while restrained as humidity was increased from ~30% to >90% RH over a period of 60–300 s to measure changes in fiber tension. The restrained fiber was then relaxed back to its original tension (15 μN) and fiber shrinkage was calculated as the change in fiber length. Our contraction testing ($N = 5$, $n = 5$) revealed weak contraction stress (5.83 ± 1.61 MPa) and shrinkage (0.72 ± 0.22%) values.

Tensile testing

Mechanical properties of capture threads from *A. tasmaniensis* individuals were determined by conducting tensile tests in low

($N = 11$, $n = 13$, 30% RH, 20°C) and high ($N = 14$, $n = 14$, >90% RH, 20°C) humidity conditions. We tested at least one sample per treatment per individual. Our methods were similar to those described by Swanson *et al.* (2007) and Blamires, Wu & Tso (2012). Samples were mounted vertically to the uppermost grips of the extension arm and force plate. The samples tested at high humidity were exposed to >90% RH for 2–5 min prior to testing, similar to previous studies as outlined above. Load-extension data were generated for capture threads pulled to breaking with an extension rate of 1.5% strain s^{-1}. True stress values were calculated from load data using the formula, $\sigma_t = F/A$, where F is force applied and A is the instantaneous cross-sectional area of the thread being tested, assuming constant volume (Guinea *et al.*, 2006). True strain values were calculated from extension data using the formula, $\varepsilon_t = \ln(L/L_0)$, where L is instantaneous gage length and L_0 is initial gage length (10 mm for all samples). Young's modulus was calculated as the initial linear slope of the stress–strain curve before yield and work to break or toughness was calculated as the area under the stress–strain curves.

On-site measurement of thread extension

We performed simple extension tests on threads in caves to assess the potential effects of drying and transit. We gently adhered the ends of threads to the tip of a bare finger and stretched the capture threads to breaking. We measured initial (L_0) and final (L_F) lengths of 25 threads from 11 individuals
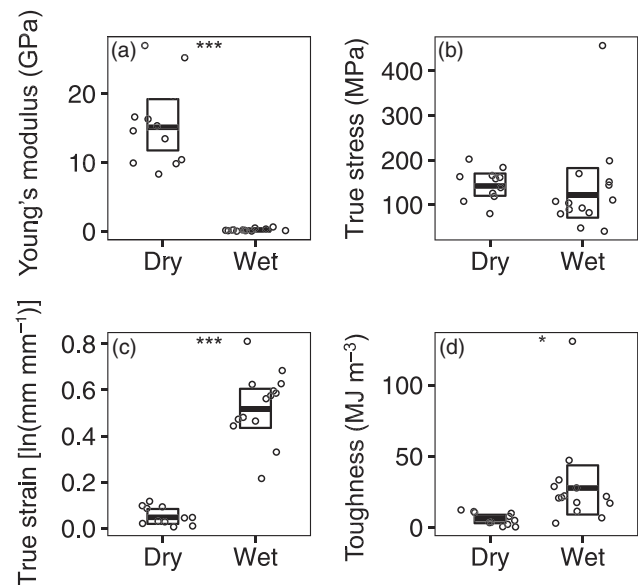

Figure 2 Polarized light microscopy image of an *Arachnocampa tasmaniensis* silk capture thread affixed to a glass microscope slide with glue dispersed by water. Two silk fibers appear in the center surrounded by dried glue residue. Scale bar length is 15 μm. [Colour figure can be viewed at zslpublications.onlinelibrary.wiley.com]

Figure 3 Mean ± 95% highest posterior density intervals for tensile properties of *Arachnocampa tasmaniensis* capture threads exposed to dry (N individuals = 11, n samples = 13, ~30% RH) and wet conditions (N = 14, n = 14, >90% RH). Significant differences between treatments are represented by stars, *** indicating significance level of $P_{MCMC} < 0.001$ and * indicating a significance level of $P_{MCMC} < 0.05$. Points represent individual averages and are offset horizontally for identification purposes.
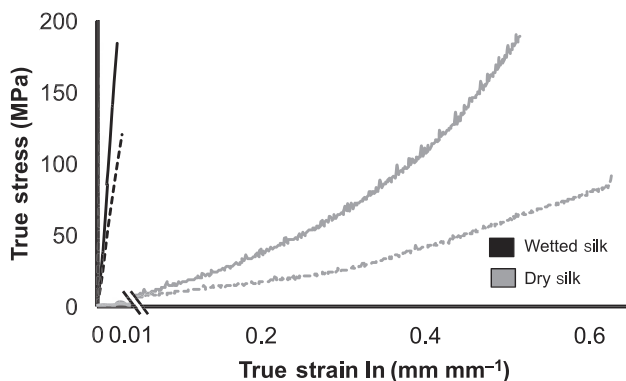
Figure 4 Representative mechanical performance of capture thread fragments exposed to low humidity (30% RH, black lines) and high humidity (>90% RH, gray lines) from two *A. tasmaniensis* larvae (one sample per treatment per individual). Similar line style (solid or dashed) indicates capture thread fragments collected from the same individual.

within the cave where humidity was at >95% RH. From these values, we calculated engineering strain of the threads as: $(L_F - L_0)/(L_0)$. We estimate strain rate for each test to be between 10% and 20% s^{-1} as stretching lasted 10–15 s. We found an average strain value of 0.28 (N individuals = 11, n samples = 25), which is <0.53 strain value we measured for thread segments in the laboratory at >90% RH (see Results, Table 2). While direct comparison between on-site and laboratory testing are not relevant because the methodologies used differed, it appears that the effects of transit and drying of silk on strain are minimal since our values attained for threads in caves did not exceed those from of the laboratory tests.

Adhesion testing

The adhesive properties of 17 capture threads from nine different *A. tasmaniensis* individuals were determined using previously described methods (Sahni, Blackledge &

Dhinojwala, 2011; Blamires *et al.*, 2014). Capture threads were mounted into the upper grips of the extension arm of the tensile tester, while a stage made of a standard glass surface was mounted into the lower grips. The fiber was lowered onto the stage and a force of 50 μN was applied for 10 seconds, thus ensuring firm and direct contact. The thread was then pulled off the stage at a rate of 0.1 mm s^{-1}. Load-displacement curves were generated as the thread detached from the glass stage and work of adhesion was calculated as the area under these curves.

For threads tested at high humidity, the tests were conducted within an airtight environmental chamber (see Agnarsson *et al.*, 2009) where relative humidity was brought to >90% about 2 min prior to testing to ensure complete hydration of the capture thread. Relative humidity was reduced to ~30% within the environmental chamber for tests conducted in dry conditions. Each sample was subjected to 1–5 replicate tests (Wet: N individuals = 9, n replicate tests = 21, Dry: N = 8, n = 18). The stage was shifted and cleaned with isopropyl alcohol after every test to ensure that the contact area with the stage was not contaminated and that no section of a thread segment was tested twice.

Statistical analysis

We used two multivariate general linear mixed models that used Markov Chain Monte Carlo (MCMC) methods to compare the mechanical and adhesive properties between wet and dry treatments. Two random factors were used in the mixed model: (1) among glow-worm individuals, which compared the differences between treatments within individuals, and (2) within individuals, to account for pseudo-replication within individuals and treatments. Parameters in mixed models were tested using 95% highest posterior density (HPD) intervals as well as MCMC P-value. Uninformative priors were specified for intercepts and fixed effects with normal distributions (mean = 0 and variance = 10^8). Uninformative priors for random factors and residuals were specified as inverse gamma distributions (shape parameter = 0.0001 and scale parameter = 0.0001). Residual variances among treatments were allowed to vary to account for potential heterogeneity. A total

Table 1 Results of mixed model tests of differences in adhesion and tensile properties of *Arachnocampa tasmaniensis* capture silk threads tested in high (>90% RH) versus low (~30% RH) humidity

Test	Property[a]	Posterior mode[b]	95% credible interval	P_{MCMC}
Adhesion	Detachment force	20.56	13.84, 28.13	**<0.001**
	Extension	2.24	1.74, 2.69	**<0.001**
	Work of adhesion	56.65	26.41, 88.61	**0.002**
Tensile	True stress	−16.88	−77.11, 39.40	0.55
	True strain	0.47	0.39, 0.56	**<0.001**
	Modulus	−15.09	−18.96, −11.52	**<0.001**
	Toughness	22.04	5.89, 40.77	**0.01**

Bold indicates significance values of $P < 0.05$.
[a]Units of measure: detachment force (μN mm^{-1}), extension (mm), work of adhesion (J $\times$ 10^{-9}) true stress (MPa), true strain ln(mm mm^{-1}), Young's modulus (GPa), toughness (MJ m^{-3}).
[b]Values indicate difference between property means of high versus low humidity treatments.

Table 2 Tensile properties of *Arachnocampa tasmaniensis* capture threads and silk of other invertebrates tested in wet and dry conditions

Common name	Order	Silk type	Species	N individuals, n samples	Treatment	Young's modulus (GPa)	True values Stress at break (MPa)	Strain at break ln(mm mm⁻¹)	Toughness (MJ m⁻³)	Reference
Glow-worm	Diptera	Capture thread	*Arachnocampa tasmaniensis*	5, 5	>90% RH	0.1 ± 0.02	122.77 ± 16.1	0.6 ± 0.04	25.82 ± 2.8	This study
Glow-worm	Diptera	Capture thread	*Arachnocampa tasmaniensis*	4, 5	30% RH	18.38 ± 2.3	159.04 ± 12.1	0.02 ± 0.01	2.4 ± 0.7	This study
Mussel	Mytiloida	Byssus	*Mytilus edulis*	–, 23	In sea water	0.85 ± 0.87	302.4	0.36	12.5 ± 10.1	Smeathers & Vincent (1979)[a]
Mussel	Mytiloida	Byssus	*Mytilus edulis*	–, 16	Dry[b]	18.69 ± 9.09	2347.4	0.19	31.5 ± 19.8	Smeathers & Vincent (1979)[a]
Mussel	Mytiloida	Byssus	*Aulacomya ater*	–, 5	Dry[b]	1.75 ± 0.26	183.73 ± 44.18	0.24	–	Troncoso et al. (2008)[a]
Mussel	Mytiloida	Byssus	*Aulacomya ater*	–, 5	In sea water	–	110.20 ± 49.40	0.61	–	Troncoso et al. (2008)[a]
Mussel	Mytiloida	Byssus	*Aulacomya ater*	–, 5	In distilled water	–	127.78 ± 50.02	0.58	–	Troncoso et al. (2008)[a]
Lacewing	Neuroptera	Eggstalk	*Chrysopa carnea*	10, 50–55	30% RH	5.8	70	0.03	1	Bauer et al. (2012)
Lacewing	Neuroptera	Eggstalk	*Chrysopa carnea*	10, 50–55	70% RH	3.2	155	2.00	97	Bauer et al. (2012)
Lacewing	Neuroptera	Eggstalk	*Chrysopa carnea*	10, 50–55	100% RH	1.3	232	4.34	110	Bauer et al. (2012)
Caddisfly	Trichoptera	Aquatic net	*Stenopsyche marmorata*	1, 1	65% RH	–	–	0.02	–	Tsukada et al. (2010)[a]
Caddisfly	Trichoptera	Aquatic net	*Stenopsyche marmorata*	1, 1	Water saturated[c]	–	–	0.41	–	Tsukada et al. (2010)[a]
Silkworm	Lepidoptera	Cocoon	*Antheraea pernyi*	–	10% RH	11.8	–	–	–	Fu et al. (2009)
Silkworm	Lepidoptera	Cocoon	*Antheraea pernyi*	–	70% RH	8.5	–	–	–	Fu et al. (2009)
Silkworm	Lepidoptera	Cocoon	*Antheraea pernyi*	–	98% RH	0.8	–	–	–	Fu et al. (2009)
Silkworm	Lepidoptera	Cocoon	*Bombyx mori*	–	Dry[b]	14	570	0.20	–	Plaza et al. (2008)
Silkworm	Lepidoptera	Cocoon	*Bombyx mori*	–	In water	3.8	450	0.27	–	Plaza et al. (2008)
Spider	Araneae	Viscid	*Argiope aurantia*	–, 17	Wet[d]	0.009 ± 0.011	1034 ± 344	1.57 ± 0.24	211 ± 99	Sensenig, Agnarsson & Blackledge, (2010)
Spider	Araneae	Viscid	*Argiope trifasciata*	–, 9	Wet[d]	0.008 ± 0.005	949 ± 292	1.44 ± 0.16	185 ± 65	Sensenig et al. (2010)
Spider	Araneae	Viscid	*Argiope argentata*	5, 87	Wet[d]	0.001 ± 0.0001	534 ± 40	1.72 ± 0.05	75 ± 6	Blackledge & Hayashi (2006)
Spider	Araneae	Viscid	*Argiope trifasciata*	–, 13	Cleaned[e]	6 ± 4	800 ± 200	0.5 ± 0.2	–	Guinea et al. (2012)
Spider	Araneae	Viscid	*Argiope trifasciata*	–, 4	Cleaned[e]	5 ± 1	800 ± 100	0.76 ± 0.08	250 ± 50	Perea et al. (2013)
Spider	Araneae	Major ampullate	*Argiope trifasciata*	2, 3	35% RH	10.7 ± 0.3	1300 ± 200	0.17 ± 0.02	90 ± 30	Guinea et al. (2012)
Spider	Araneae	Major ampullate	*Argiope trifasciata*	2, 3	In water	0.022 ± 0.001	1420 ± 50	0.95 ± 0.03	185 ± 8	Guinea et al. (2012)

Table 2 Continued.

Common name	Order	Silk type	Species	N individuals, n samples	Treatment	Young's modulus (GPa)	True values Stress at break (MPa)	Strain at break ln(mm mm⁻¹)	Toughness (MJ m⁻³)	Reference
Spider	Araneae	Major ampullate	Nephila inaurata	2, 3	35% RH	14.2 ± 0.6	1800 ± 60	0.26 ± 0.01	264 ± 5	Guinea et al. (2012)
Spider	Araneae	Major ampullate	Nephila inaurata	2, 3	In water	0.041 ± 0.004	1700 ± 100	0.67 ± 0.01	280 ± 10	Guinea et al. (2012)
Spider	Araneae	Major ampullate	Araneus diadematus	5, 25–50	25% RH	7.8 ± 0.8	688 ± 44	0.10 ± 0.02	–	Shao et al. (1999)[a]
Spider	Araneae	Major ampullate	Araneus diadematus	5, 25–50	In water	~0.1	845 ± 65	0.26 ± 0.03	–	Shao et al. (1999)[a]
Spider	Araneae	Major ampullate	Argiope trifasciata	1, 2	~15% RH	~10	~1300	~0.26	–	Plaza et al. (2006)
Spider	Araneae	Major ampullate	Argiope trifasciata	1, 2	~100% RH	~0.03	~725	~1.06	–	Plaza et al. (2006)
Spider	Araneae	Cribellate axial	Hyptiotes cavatus	7, 23	~30% RH	3.4 ± 0.48	577 ± 58	0.29 ± 0.03	78 ± 8	Piorkowski & Blackledge (2017)
Spider	Araneae	Cribellate axial	Hyptiotes cavatus	6, 20	>90% RH	0.2 ± 0.02	709 ± 196	0.36 ± 0.02	77 ± 20	Piorkowski & Blackledge (2017)
Spider	Araneae	Cribellate axial	Uloborus plumipes	3, 6	~30% RH	0.47 ± 0.21	237 ± 49	0.37 ± 0.08	31 ± 12	Piorkowski & Blackledge (2017)
Spider	Araneae	Cribellate axial	Uloborus plumipes	3, 7	~90% RH	0.12 ± 0.05	194 ± 52	0.42 ± 0.02	21 ± 5	Piorkowski & Blackledge (2017)
Spider	Araneae	Minor ampullate	Nephila inaurata	2, 3	35% RH	11.2 ± 0.7	1500 ± 200	0.46 ± 0.05	300 ± 50	Guinea et al. (2012)
Spider	Araneae	Minor ampullate	Nephila inaurata	2, 3	In water	0.39 ± 0.03	1000 ± 100	0.53 ± 0.09	210 ± 60	Guinea et al. (2012)
Spider	Araneae	Minor ampullate	Argiope trifasciata	2, 3	35% RH	10 ± 0.4	1040 ± 60	0.45 ± 0.02	240 ± 20	Guinea et al. (2012)
Spider	Araneae	Minor ampullate	Argiope trifasciata	2, 3	In water	1.42 ± 0.09	1220 ± 200	0.51 ± 0.01	245 ± 25	Guinea et al. (2012)

Values reported as mean ± SEM (SD for Troncoso et al., 2008, Sensenig et al. 2010), when applicable or as (~) mean approximations from reference figures/text. (–) Data not available.

[a]True values calculated from engineering values.

[b]Samples tested at ambient humidity (20–70% RH).

[c]Sample tested after saturation in water for 10 h.

[d]Untreated samples tested in ambient conditions.

[e]Aggregate glue coating of viscid silk removed via centrifugation.

of 2 600 000 MCMC iterations were simulated including initial 100 000 burn-in iterations followed by 2 500 000 iterations with a 500× thinning rate.

Results

Mechanical performance

The tensile performance of *A. tasmaniensis* capture threads was significantly different in high humidity (>90% RH, N individuals = 11, n samples = 13) compared to low humidity (~30% RH, N = 14, n = 14; Figs 3 and 4, Tables 1 and 2). Capture threads tested in dry conditions were brittle and stiff, showing very little extension and exhibiting only a linear stress response to increased strain with a high modulus (Fig. 3). Threads tested at high humidity were highly extensible and compliant, with the stress–strain curve displaying an initially linear slope, followed by an exponentially increasing slope, signifying strain-hardening, before eventual failure around 134 MPa stress and 53% strain (Fig. 3).

Statistical comparison between capture threads tested in high humidity versus low humidity showed that breaking strength did not differ (95% HPD intervals = −77.11 to 39.40 MPa, P_{MCMC} = 0.55, Fig. 4b, Table 1), breaking strain increased nearly 30-fold (95% HPD intervals = 0.39–0.56, P_{MCMC} < 0.001, Fig. 4c, Table 1), toughness increased by an order of magnitude (95% HPD intervals = 5.89–40.77 MJ 10^{-9}, P_{MCMC} < 0.001, Fig. 4d, Table 1) and Young's modulus decreased by two orders of magnitude (95% HPD intervals = −18.96 to −11.52 GPa, P_{MCMC} < 0.001, Fig. 4a, Table 1).

Adhesive properties

We found that the adhesive properties of *A. tasmaniensis* capture threads improved in high humidity conditions (>90% RH, N individuals = 9, n replicate tests = 21) compared to low humidity (~30% RH, N = 8, n = 18) conditions (Figs 5 and 6, Tables 1 and 3). Our adhesion tests showed that the dry capture threads tested in low humidity were mostly non-adhesive as values for detachment extension, force and work were close to zero (mean ± SE: force of adhesion: 0.25 ± 0.07 μN mm^{-1}, extension at detachment: 0.14 ± 0.006 mm, work of adhesion: 0.006 ± 0.002 J × 10^{-9}, Fig. 6, Table 3). However, capture threads tested in high humidity showed much greater adhesion (force of adhesion: 23.66 ± 4.59 μN mm^{-1}, extension at detachment: 2.48 ± 0.28 mm, work of adhesion 64.86 ± 19.69 J × 10^{-9}, Fig. 6, Table 3) during pull-off tests. Detachment extension, force, and work of adhesion of capture threads tested in high humidity were both significantly greater than those tested in dry conditions by multiple orders of magnitude (Fig. 5, Table 1, force of adhesion: 95% HPD intervals = 13.84–28.13 μN mm^{-1}, P_{MCMC} < 0.001, extension at detachment: 95% HPD intervals = 1.74–2.69 mm, P_{MCMC} < 0.001, work of adhesion: 95% HPD intervals = 26.41–88.61 J × 10^{-9}, P_{MCMC} = 0.002).
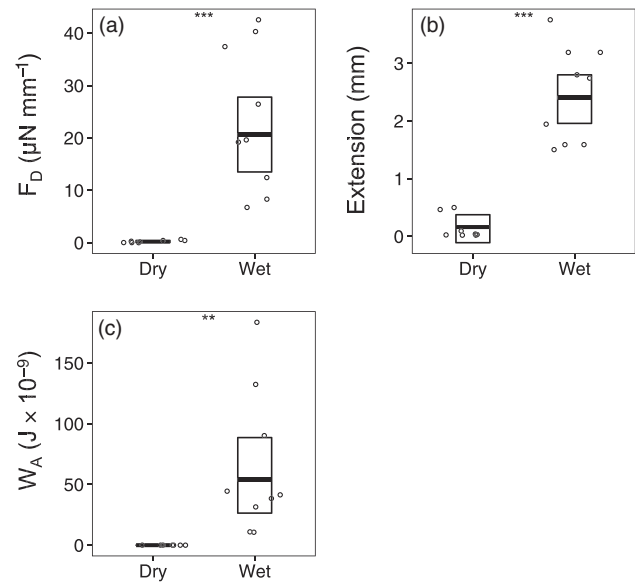
Figure 5 Mean ± 95% highest posterior density intervals for force at detachment (a), extension at detachment (b) and work of adhesion (c) of *Arachnocampa tasmaniensis* capture threads exposed to dry (N individuals = 8, n samples = 18–30% RH) and wet conditions (N = 9, n = 21, >90% RH). Significant differences between treatments are represented by horizontal lines with *** indicating significance level of P_{MCMC} < 0.001 and ** indicating significance level of P_{MCMC} < 0.01. Points represent individual averages and are offset horizontally for identification purposes.
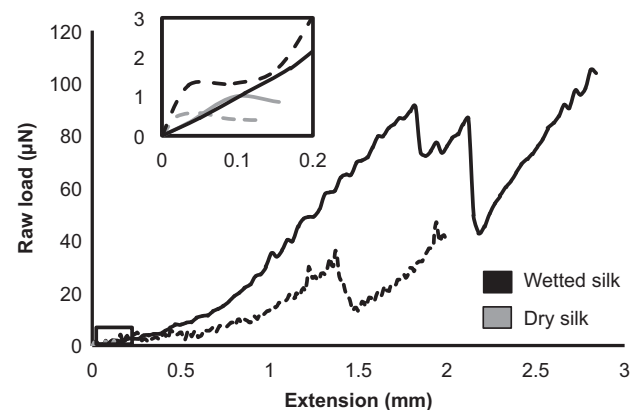
Figure 6 Four representative force-extension curves from pull-off tests of a single *A. tasmaniensis* capture thread fragment adhering to a force plate in dry (30% RH, gray lines) and wet conditions (90%RH, black lines). Solid lines represent the first test of a given treatment and dashed lines represent the second. Sharp peaks indicate partial detachment of thread from test substrate with the end of the curve indicating complete detachment.

Table 3 Adhesive properties of glow-worm and spider capture threads in different humidities

Common name	Order	Silk type	Species	N individuals, n samples	Humidity (% RH)	Extension (mm)	Force at detachment (µN mm^{-1})	Work of adhesion (J × 10^{-9})	Reference[a]
Glow-worm	Diptera	Capture thread	Arachnocampa tasmaniensis	9, 21	>90	2.48 ± 0.28	23.66 ± 4.59	64.86 ± 19.69	This study
Glow-worm	Diptera	Capture thread	Arachnocampa tasmaniensis	8, 18	30	0.14 ± 0.006	0.25 ± 0.07	0.006 ± 0.002	This study
Spider	Araneae	Viscid	Argiope aurantia	14, –	20	0.50	523.25	–	Opell et al. (2013)
Spider	Araneae	Viscid	Argiope aurantia	14, –	37	1.75	150.8	–	Opell et al. (2013)
Spider	Araneae	Viscid	Argiope aurantia	14, –	55	2.90	52.3	–	Opell et al. (2013)
Spider	Araneae	Viscid	Argiope aurantia	14, –	72	3.30	61.49	–	Opell et al. (2013)
Spider	Araneae	Viscid	Argiope aurantia	14, –	90	4.25	36.1	–	Opell et al. (2013)
Spider	Araneae	Viscid	Neoscona crucifera	14, –	20	<0.1	–	–	Opell et al. (2013)
Spider	Araneae	Viscid	Neoscona crucifera	14, –	37	0.20	347.2	–	Opell et al. (2013)
Spider	Araneae	Viscid	Neoscona crucifera	14, –	55	0.45	522.48	–	Opell et al. (2013)
Spider	Araneae	Viscid	Neoscona crucifera	14, –	72	1.30	425.42	–	Opell et al. (2013)
Spider	Araneae	Viscid	Neoscona crucifera	14, –	90	4.10	548.68	–	Opell et al. (2013)
Spider	Araneae	Viscid	Cyrtarachne bufo	2, 14	100	–	90	–	Baba et al. (2014)
Spider	Araneae	Viscid	Cyrtarachne bufo	2, 14	60	–	19	–	Baba et al. (2014)
Spider	Araneae	Viscid	Cyrtarachne akirai	3, 20	100	–	81	–	Baba et al. (2014)
Spider	Araneae	Viscid	Cyrtarachne akirai	3, 22	60	–	14	–	Baba et al. (2014)
Spider	Araneae	Viscid	Cyrtarachne nagasakiensis	3, 15	100	–	55	–	Baba et al. (2014)
Spider	Araneae	Viscid	Cyrtarachne nagasakiensis	3, 13	60	–	18	–	Baba et al. (2014)
Spider	Araneae	Viscid	Larinia argiopiformis	8, 44	100	–	28	–	Baba et al. (2014)
Spider	Araneae	Viscid	Larinia argiopiformis	8, 44	60	–	26	–	Baba et al. (2014)
Spider	Araneae	Viscid	Larinioides cornutus	–, 10	0	–	3	80	Sahni et al. (2014)
Spider	Araneae	Viscid	Larinioides cornutus	–, 10	100	–	160	310	Sahni et al. (2014)
Spider	Araneae	Viscid	Larinioides cornutus	–, 5	15	0.04	200	16	Sahni et al. (2011)
Spider	Araneae	Viscid	Larinioides cornutus	–, 5	40	0.21	220	64	Sahni et al. (2011)
Spider	Araneae	Viscid	Larinioides cornutus	–, 5	90	0.14	205	48	Sahni et al. (2011)
Spider	Araneae	Gumfoot	Latrodectus hesperus	–, 5	15	0.08	50	7	Sahni et al. (2011)
Spider	Araneae	Gumfoot	Latrodectus hesperus	–, 5	40	0.09	35	6	Sahni et al. (2011)
Spider	Araneae	Gumfoot	Latrodectus hesperus	–, 5	90	0.08	30	7	Sahni et al. (2011)
Spider	Araneae	Gumfoot	Latrodectus hesperus	–, 15	10	–	–	40	Jain et al. (2015)
Spider	Araneae	Gumfoot	Latrodectus hesperus	–, 15	30	–	–	590	Jain et al. (2015)
Spider	Araneae	Gumfoot	Latrodectus hesperus	–, 15	50	–	–	500	Jain et al. (2015)
Spider	Araneae	Gumfoot	Latrodectus hesperus	–, 15	70	–	–	590	Jain et al. (2015)
Spider	Araneae	Gumfoot	Latrodectus hesperus	–, 15	90	–	–	600	Jain et al. (2015)

Values reported as mean ± SEM. (–) Data not available.

[a]Data from references is approximated from figures and force values from Opell et al. (2013) were calculated from stress values.

Discussion

Rubberization of capture thread axial fibers

Our tensile experiments revealed that *A. tasmaniensis* capture threads are brittle and glassy when dry but rubbery and extensible when wetted by high humidity (Figs 3 and 4). This transition from glassy to rubbery mechanical behavior has been demonstrated in many amorphous protein and sugar-based biomolecules (Mathew & Dufresne, 2002; Blasi *et al.*, 2005; Vollrath & Porter, 2006; Cordone *et al.*, 2007) as the material is exposed to a temperature above the glass transition threshold (T_g). By promoting molecular mobility, water can greatly reduce T_g as water is a known plasticizer (Sperling, 2005). While we did not ascertain the T_g of dried glow-worm capture threads, we can assume exposure to high humidity reduced T_g to at least room temperature (20°C) in our samples.

The plasticization effect of water has been previously demonstrated in silks from several other invertebrates (Table 2). Silks produced by animals that live underwater, such as attachment byssus of *Mytilus* and *Aulacomya* mussels and net silk of the caddisfly *Stenopsyche marmorata*, can be an order of magnitude stiffer and up to an order of magnitude less extensible when dry (Table 2). The silk of some terrestrial arthropods may also be affected by water in a similar way. The cocoon silk of *Bombyx mori* and *Antheraea pernyi* and minor ampullate and cribellate axial silk of several orb web spiders display a 1–2 order of magnitude decrease in initial modulus (Table 2). However, orb web spider viscid capture silk and major ampullate silk and lacewing (*Chrysopa carnea*) egg stalk silk show the greatest change in property when exposed to water, displaying a 1–3 order of magnitude increase in compliance and 1–2 order of magnitude increase in extensibility (Table 2).

Disruption of hydrogen bonds (H-bonds) has been proposed as the primary mechanism for how these silks deform in the presence of water (Termonia, 1994; Bauer *et al.*, 2012). In some cases, such as lacewing silk, intermolecular H-bonds are disrupted in the crystallite regions of the silk (Bauer *et al.*, 2012) causing cross-β-sheet crystals to unravel and extend. In other cases, such as silkworm and spider silks, the H-bond lattice within the silk's amorphous region is disrupted promoting molecular mobility (Work & Morosoff, 1982; Termonia, 1994; Grubb & Ji, 1999; Eles & Michal, 2004), facilitating fiber contraction up to 50% in some spider silks (Boutry & Blackledge, 2010). We can only speculate here on the role of H-bonds in *A. tasmaniensis* capture threads in determining its mechanical behavior. We only detected marginal contraction of fibers exposed to high humidity ($N = 5$, $n = 5$, $0.72 \pm 0.22\%$), which does not provide strong evidence for an interconnected H-bond lattice. However, previous studies have revealed a complex combination of cross-β-sheet crystals, similar to lacewing silk, a low crystal fraction, similar to spider major ampullate silk, and the presence of a highly disordered amorphous region (Walker *et al.*, 2015). Further studies are clearly needed to determine the molecular mechanisms affecting the performance of these unique silks.

Capture thread adhesion

Biological adhesives that capture prey, such as velvet worm slime and spider glue, utilize water to enhance interfacial adhesion by facilitating the spreading of adhesive macromolecules and preventing excessive cohesion (Haritos *et al.*, 2010; Opell *et al.*, 2013; Amarpuri *et al.*, 2015). For example, spiders use glue-coated viscid threads, which are functionally analogous to glow-worm capture threads, to entrap prey in their webs (Blackledge, Kuntner & Agnarsson, 2011; Foelix, 2011). These silks can remain sticky in variable environments but seem to be optimized for certain humidity levels (Opell *et al.*, 2013; Baba *et al.*, 2014; Amarpuri *et al.*, 2015). Several species of *Cyrtarachne* spiders, specialized moth-catching orb web weavers, and *Tetragnatha laboriosa*, orb web spiders that live near water, require very high humidity (100% RH) or face a three- to sevenfold decrease in stickiness (Baba *et al.*, 2014; Amarpuri *et al.*, 2015).

Our adhesion experiments reveal that *A. tasmaniensis* capture threads displayed a three order of magnitude increase in adhesive force and five order of magnitude increase in work of adhesion when tested at high humidity (100% RH) compared to low humidity (30% RH, Fig. 6, Tables 1 and 3). The glue droplets from the capture threads of three species of *Arachnocampa* (including *A. tasmaniensis*) were previously observed to crystallize at humidity levels <80% (RH), also indicating a strong effect of drying on the glue (Von Byern *et al.*, 2016). While we did not ascertain whether adhesion changes gradually or instantly at some critical value, our results clearly show that the high humidity of caves and cave-like environments is required to facilitate glow-worm silk adhesion.

Conclusions

We demonstrated that *A. tasmaniensis* capture threads were more extensible, compliant and tougher with greater adhesiveness in high humidity (>90% RH) compared to lower humidity (30% RH). We infer our results as indicative of water inducing: (1) plasticization of the glow-worm silk fiber by water, and (2) solvation and spreading of hygroscopic biomolecules in the glue. Our results indicate that the water-facilitated increase in thread adhesion and mechanical toughness in *A. tasmaniensis* capture threads has biological consequences. We showed that low humidity renders their sticky silk threads ineffective for prey capture. Accordingly, we expect that these animals are likely restricted to foraging in high humidity habitats, such as wet caves and adjacent forests.

Acknowledgements

References

Agnarsson, I., Boutry, C., Wong, S.C., Baji, A., Dhinojwala, A., Sensenig, A.T. & Blackledge, T.A. (2009). Supercontraction forces in spider dragline silk depend on hydration rate. *Zoology* **112**, 325–331.

Amarpuri, G., Zhang, C., Diaz, C., Opell, B.D., Blackledge, T.A. & Dhinojwala, A. (2015). Spiders tune glue viscosity to maximize adhesion. *ACS Nano* **9**, 11472–11478.

Baba, Y.G., Kusahara, M., Maezono, Y. & Miyashita, T. (2014). Adjustment of web-building initiation to high humidity: a constraint by humidity-dependent thread stickiness in the spider *Cyrtarachne*. *Naturwissenschaften* **101**, 587–593.

Bauer, F., Bertinetti, L., Masic, A. & Scheibel, T. (2012). Dependence of mechanical properties of lacewing egg stalks on relative humidity. *Biomacromoleucles* **13**, 3730–3735.

Blackledge, T.A. & Hayashi, C.Y. (2006). Silken toolkits: biomechanics of silk fibers spun by the orb web spider *Argiope argentata* (Fabricius 1775). *J. Exp. Biol.* **209**, 2452–2461.

Blackledge, T.A., Cardullo, R.A. & Hayashi, C.Y. (2005). Polarized light microscopy, variability in spider silk diameters, and the mechanical characterization of spider silk. *Invertebr. Biol.* **124**, 165–173.

Blackledge, T.A., Kuntner, M. & Agnarsson, I. (2011). The form and function of spider orb webs: evolution from silk to ecosystems. *Adv. Insect Physiol.* **41**, 175.

Blamires, S.J., Wu, C.L. & Tso, I.M. (2012). Variation in protein intake induces variation in spider silk expression. *PLoS ONE* **7**, e31626.

Blamires, S.J., Sahni, V., Dhinojwala, A., Blackledge, T.A. & Tso, I.M. (2014). Nutrient deprivation induces property variations in spider gluey silk. *PLoS ONE* **9**, e88487.

Blasi, P., D'souza, S.S., Selmin, F. and DeLuca, P.P. 2005. Plasticizing effect of water on poly (lactide-co-glycolide). *J. Control. Release* **108**: 1–9.

Boutry, C. & Blackledge, T.A. (2010). Evolution of supercontraction in spider silk: structure–function relationship from tarantulas to orb-weavers. *J. Exp. Biol.* **213**, 3505–3514.

Broadley, R.A. & Stringer, I.A. (2001). Prey attraction by larvae of the New Zealand glow-worm, *Arachnocampa luminosa* (Diptera: Mycetophilidae). *Invertebr. Biol.* **120**, 170–177.

Cordone, L., Cottone, G. & Giuffrida, S. (2007). Role of residual water hydrogen bonding in sugar/water/biomolecule systems: a possible explanation for trehalose peculiarity. *J. Phys. Condens. Matter* **19**, 205110.

Eles, P.T. & Michal, C.A. (2004). Strain dependent local phase transitions observed during controlled supercontraction reveal mechanisms in spider silk. *Macromolecules* **37**, 1342–1345.

Foelix, R.F. (2011). *Biology of spiders*. 3rd edn. Oxford: Oxford University Press.

Fu, C., Porter, D. & Shao, Z. (2009). Moisture effects on *Antheraea pernyi* silk's mechanical property. *Macromolecules* **42**, 7877–7880.

Gosline, J.M., Denny, M.W. & DeMont, M.E. (1984). Spider silk as rubber. *Nature* **309**, 551–552.

Grubb, D.T. & Ji, G. (1999). Molecular chain orientation in supercontracted and re-extended spider silk. *Int. J. Biol. Macromol.* **24**, 203–210.

Guinea, G.V., Pérez-Rigueiro, J., Plaza, G.R. & Elices, M. (2006). Volume constancy during stretching of spider silk. *Biomacromolecules* **7**, 2173–2177.

Guinea, G.V., Elices, M., Plaza, G.R., Perea, G.B., Daza, R., Riekel, C., Agulló-Rueda, F., Hayashi, C., Zhao, Y. & Pérez-Rigueiro, J. (2012). Minor ampullate silks from *Nephila* and *Argiope* spiders: tensile properties and microstructural characterization. *Biomacromolecules* **13**, 2087–2098.

Haritos, V.S., Niranjane, A., Weisman, S., Trueman, H.E., Sriskantha, A. & Sutherland, T.D. (2010). Harnessing disorder: onychophorans use highly unstructured proteins, not silks, for prey capture. *Proc. R. Soc. B Biol. Sci.* **277**, 3255–3263.

Jain, D., Zhang, C., Cool, L.R., Blackledge, T.A., Wesdemiotis, C., Miyoshi, T. & Dhinojwala, A. (2015). Composition and function of spider glues maintained during the evolution of cobwebs. *Biomacromolecules* **16**, 3373–3380.

Jelinski, L.W., Blye, A., Liivak, O., Michal, C., LaVerde, G., Seidel, A., Shah, N. & Yang, Z. (1999). Orientation, structure, wet-spinning, and molecular basis for supercontraction of spider dragline silk. *Int. J. Biol. Macromol.* **24**, 197–201.

Mathew, A.P. & Dufresne, A. (2002). Plasticized waxy maize starch: effect of polyols and relative humidity on material properties. *Biomacromolecules* **3**, 1101–1108.

Merritt, D.J. & Patterson, R. (2017). The effect of environmental conditions on the bioluminescence display of the glowworm, *Arachnocampa flava* (Diptera: Keroplatidae). *Aust. Entomol.* **57**, 107–117. https://doi.org/10.1111/aen.12274

Meyer-Rochow, V.B. (2007). Glow-worms: a review of *Arachnocampa* spp. and kin. *Luminescence* **22**, 251–265.

Opell, B.D., Karinshak, S.E. & Sigler, M.A. (2013). Environmental response and adaptation of glycoprotein glue within the droplets of viscous prey capture threads from araneoid spider orb-webs. *J. Exp. Biol.* **216**, 3023–3034.

Perea, G.B., Riekel, C., Guinea, G.V., Madurga, R., Daza, R., Burghammer, M., Hayashi, C., Elices, M., Plaza, G.R. & Pérez-Rigueiro, J. (2013). Identification and dynamics of polyglycine II nanocrystals in *Argiope trifasciata* flagelliform silk. *Sci. Rep.* **3**, 3061.

Pérez-Rigueiro, J., Viney, C., Llorca, J. & Elices, M. (2000). Mechanical properties of silkworm silk in liquid media. *Polymer* **41**, 8433–8439.

Piorkowski, D. & Blackledge, T.A. (2017). Punctuated evolution of viscid silk in spider orb webs supported by mechanical behavior of wet cribellate silk. *Sci. Nat.* **104**, 67.

Plaza, G.R., Guinea, G.V., Pérez-Rigueiro, J. & Elices, M. (2006). Thermo-hygro-mechanical behavior of spider dragline silk: glassy and rubbery states. *J. Polym. Sci. B Polym. Phys.* **44**, 994–999.

Plaza, G.R., Corsini, P., Pérez-Rigueiro, J., Marsano, E., Guinea, G.V. & Elices, M. (2008). Effect of water on *Bombyx mori* regenerated silk fibers and its application in modifying their mechanical properties. *J. Appl. Polym. Sci.* **109**, 1793–1801.

Pugsley, C. (1984). Ecology of the New Zealand glow-worm, *Arachnocampa luminosa* (Diptera: Keroplatidae), in the glow-worm cave, Waitomo. *J. R. Soc. N. Z.* **14**, 387–407.

Sahni, V., Blackledge, T.A. & Dhinojwala, A. (2011). Changes in the adhesive properties of spider aggregate glue during the evolution of cobwebs. *Sci. Rep.* **1**, 41.

Sahni, V., Miyoshi, T., Chen, K., Jain, D., Blamires, S.J., Blackledge, T.A. & Dhinojwala, A. (2014). Direct solvation of glycoproteins by salts in spider silk glues enhances adhesion and helps to explain the evolution of modern spider orb webs. *Biomacromolecules* **15**, 1225–1232.

Sensenig, A., Agnarsson, I. & Blackledge, T.A. (2010). Behavioural and biomaterial coevolution in spider orb webs. *J. Evol. Biol.* **23**, 1839–1856.

Shao, Z., Young, R.J. & Vollrath, F. (1999). The effect of solvents on spider silk studied by mechanical testing and single-fibre Raman spectroscopy. *Int. J. Biol. Macromol.* **24**, 295–300.

Smeathers, J.E. & Vincent, J.F.V. (1979). Mechanical properties of mussel byssus threads. *J. Molluscan Stud.* **45**, 219–230.

Sperling, L.H. (2005). *Introduction to polymer science*. 4th edn. Hoboken, NJ, USA: John Wiley & Sons Inc.

Swanson, B.O., Blackledge, T.A. & Hayashi, C.Y. (2007). Spider capture silk: performance implications of variation in an exceptional biomaterial. *J. Exp. Zool. Part A* **307**, 654–666.

Termonia, Y. (1994). Molecular modeling of spider silk elasticity. *Macromolecules* **27**, 7378–7381.

Troncoso, O.P., Torres, F.G. & Grande, C.J. (2008). Characterization of the mechanical properties of tough biopolymer fibres from the mussel byssus of *Aulacomya ater*. *Acta Biomater.* **4**, 1114–1117.

Tsukada, M., Khan, M.M.R., Inoue, E., Kimura, G., Hun, J.Y., Mishima, M. & Hirabayashi, K. (2010). Physical properties and structure of aquatic silk fiber from *Stenopsyche marmorata*. *Int. J. Biol. Macromol.* **46**, 54–58.

Vollrath, F. & Porter, D. (2006). Spider silk as a model biomaterial. *Appl. Phys. A* **82**, 205–212.

Von Byern, J., Dorrer, V., Merritt, D.J., Chandler, P., Stringer, I., Marchetti-Deschmann, M., McNaughton, A., Cyran, N., Thiel, K., Noeske, M. & Grunwald, I. (2016). Characterization of the fishing lines in Titiwai (=*Arachnocampa luminosa* (Skuse, 1890) from New Zealand and Australia. *PLoS ONE* **11**, e0162687.

Walker, A.A., Weisman, S., Trueman, H.E., Merritt, D.J. & Sutherland, T.D. (2015). The other prey-capture silk: fibres made by glow-worms (Diptera: Keroplatidae) comprise cross-β-sheet crystallites in an abundant amorphous fraction. *Comp. Biochem. Phys. B* **187**, 78–84.

Willis, R.E., White, C.R. & Merritt, D.J. (2011). Using light as a lure is an efficient predatory strategy in *Arachnocampa flava*, an Australian glow-worm. *J. Comp. Phys. B* **181**, 477–486.

Work, R.W. & Morosoff, N. (1982). A physico-chemical study of the supercontraction of spider major ampullate silk fibers. *Text. Res. J.* **52**, 349–356.